

Autonomous Vision-based Navigation of the Nanokhod Rover

Bernhard-Michael Steinmetz, Klaus Arbter, Bernhard Brunner, Klaus Landzettel

DLR Oberpfaffenhofen
Institute of Robotics and Mechatronics
D-82234 Wessling, Germany
Michael.Steinmetz@dlr.de

Keywords mobile vehicle, navigation, image processing, model-based localization, autonomous motion control, path planning, planetary exploration

Abstract

This paper describes an end-to-end control method for autonomous navigation of a small vehicle at a remote place, e.g. in space for planetary exploration. Due to a realistic background of this study the proposed method has to deal with limited knowledge about the environment as well as limited system resources and operational boundary conditions, e.g. very large time delay in the communication between the ground control station and the space segment. To overcome these constraints the remote system has to act in a very autonomous way. Ground support minimizes the computational load of the remote system. High-level information interchange reduces the needs in communication bandwidth.

1 Introduction

Autonomous planetary exploration will play an important role in future space missions. After the success of the Mars Pathfinder Mission [1] a lot of work has been started to overcome typical limitations of mobile vehicles [2][3][4], e.g. the lack of local autonomy at the Sojourner mission. Due to a very large time delay concerning the data link between ground and space segment (approx. 20 min transit time) and typical limitations of communication bandwidth in space, on-line control is not feasible. That means, the Rover motion commands have to be formulated at a very abstract level: In our approach a list of way-points, determined by a path planner on-ground [12][13], will be uploaded to the space segment for autonomous execution on site. Whereas most of the efforts has been done in the field of path planning [5][12], the need of an on-line navigation technique based on mission specific components has not been discussed in depth so far. To fulfil this gap, a mission scenario has been designed for this study, which focuses on the autonomous motion control of a small Rover vehicle [6]. The essential element to achieve this

autonomy is the precise localization of the Rover without advice from ground and the capability to cope with non-nominal situations by itself. Due to unknown parameters, e.g. soil characteristics, a dead reckoning approach, based for example only on odometry data, will fail. To track the Rover on its way, a more robust 3D-localization technique is necessary. In this feasibility study we propose a vision based approach for Rover localization and guidance by a stationary Lander module. A cyclical monitoring of the Rover pose and an appropriate interaction between Rover and Lander forms the basis for reaching the desired target position autonomously. The proposed methodology has to refrain from adding components to the system setup which are to the debit of anything else, e.g. scientific equipment.

2 The PSPE Project

Within the European 'Payload Support for Planetary Exploration (PSPE)' project a Lander based spacecraft configuration is proposed, which is intended to perform geo-science operations e.g. on Mars. It consists of the following components (Figure 1):

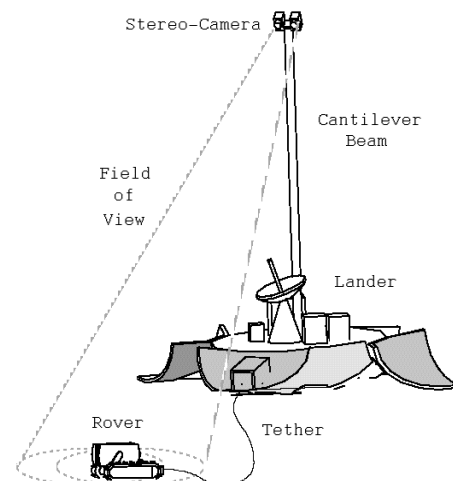


Figure 1: Lander system with Imaging Head and Nanokhod Rover

- The ‘Lander system (LS)’ carries both all of the supply engineering and the complete control system for the Rover, the scientific instrumentation and the communication with the ‘Ground Control Station (GCS)’. Depending on the mission additional scientific equipment can be integrated.
- The ‘Imaging Head (IH)’ (Figure 2, Table 1), mounted on top of a vertical cantilever beam coming out of the LS, is an inherent part of the scientific payload. This IH is equipped with a space-applicable stereo camera technique, and for all around site investigation with a two degrees of freedom ‘Pan and Tilt Unit (PTU)’. The cameras are optimized for both taking stereoscopic panorama-images of the landing site and the detection of interesting objects around the LS. Due to the strong accuracy requirements a high-fidelity camera calibration is performed at the manufacturer’s site.
- The ‘Nanokhod-Rover (NR)’ is a rugged, simple, reliable yet effective, track-driven carrier of scientific equipment (Figure 3, Table 2), optimized to transport them to interesting points in the vicinity of the LS, and to carry out in-situ measurements [7][11]. Tethered to the LS via a power and data cable the NR benefits from the LS supply engineering. This joint use results in a very high payload- to total-mass ratio of the NR. But on the other hand it limits the operational range to a maximum distance of approx. 20 meters around the LS. The NR itself is equipped with four degrees of freedom (two for locomotion and two for ‘payload-cabin (PLC)’ alignment).

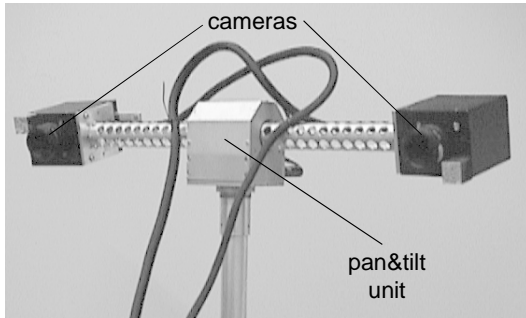


Figure 2: IH with PTU and stereoscopic camera system

Stereo camera	Focus	fix at 20 m distance
	Resolution	1024 x 1024 pixel
	Field of View	23° x 23°
	CCD pixel size	14µm x 14µm
	Stereo-base	0.5 m
	Vergence	5° for each camera
Pan Unit	Accuracy	+/- 0.94 arc-minutes
Tilt Unit	Accuracy	+/- 0.465 arc-minutes

Table 1: IH Characteristics

The PSPE GCS [13] provides an easy-to-use command interface, optimized for intuitive scientific experiment support without the need to have specific knowledge in the field of robotics. The base for all is a terrain model reconstructed on-ground from the stereoscopic panorama-images taken by the IH during all around landing site exploration. A mission specialist selects interesting sites or objects in the terrain model, to be explored by the NR – the so called ‘long arm’ of the LS. A sophisticated path planning algorithm determines the optimal path with careful attention to given constraints (e.g. topography, estimated soil and known NR characteristics) [8][12].

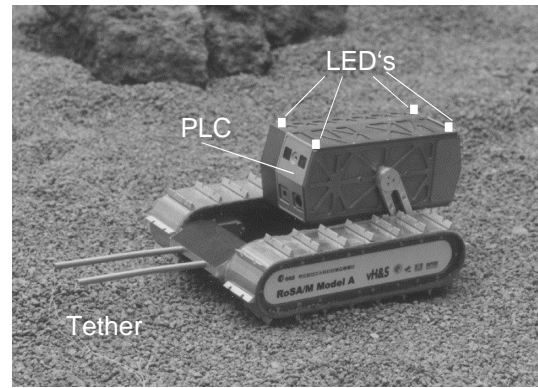


Figure 3: The NR with raised payload cabin (PLC).

Size (LxWxH)	max. 340 x 165 x 130 mm
Weight	1450 g (rover) + 1100 g (payload)
Tether length	100 m
Degree of freedom	4 (2 locomotion, 2 payload cabin)
Speed (tracks)	approx. 1.4 mm/sec
Size of LED	3.0 x 3.0 mm

Table 2: NR Characteristics

The following chapters focus on the autonomous navigation aspect based on a predefined list of way point at the LS.

3 Navigation

The navigation task is characterized by the following features: Due to the usage of a tether the NR freedom of action is hard-limited. Due to a NR-dimension to surface-structure ratio of approx. 1:1 the path control is dominated by discontinuities which abruptly affects the motion behaviour in an unpredictable way. Due to limited computational power and severe requirements in simplicity and robustness the localization method is based on an active marker concept for vision-based evaluation.

Besides, the unknown interaction between the tracks of the NR and the local soil has an unpredictable impact on

any command execution, especially for rotations. Although a fix and undisturbed constellation exists between the planned way points and the LS, it is not possible to define a precise mathematical model of the path which fits all of the required characteristics in advance. And finally the formation of the heterogeneous topology, which has to be passed by the NR, strongly depends on the direction of motion and cannot be extrapolated on information out of a motion history. Due to those constraints and a mission specific separation of the system into exclusive path planning on ground (GCS) and autonomous navigation on board (LS), the planning operation has to identify extra space for a local refinement of any planned motion.

3.1 Path segment classification

As mentioned before, each path consists of a list of way points. Two consecutive way points mark a path segment. Each path is build up of a finite number of path segments. Due to the lack of creating a precise path model, the space around each path segment has to be roughly classified using apriori knowledge of the controlled system (e.g. characteristics of NR and identified terrain) [8]. This firm segmentation marks a region of allowed autonomous activities (Figure 4: Space between On- and Off-track margin).

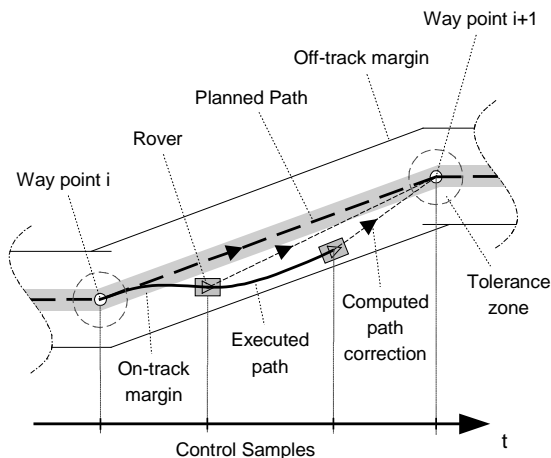


Figure 4: Path segment segmentation

On the other hand, within the On-track margin no intervention is necessary and outside of the Off-track margin any autonomous correction is forbidden due to an incalculable risk. Per definition each path, which does not violate the Off-track margin, is equivalent to the original planned path.

3.2 In-situ classification of actual facts

In addition to tracing the superior navigation goal, 'In-Situ Classification (ISC)' analyses the NR behaviour in principle. It is mandatory for any local autonomy, which has to deal with unmodeled path execution events, to

identify the history as well as the impact of problems wrt. the desired navigation goal in order to compensate them. A well-proven method to uncover discrepancies is an on-line 'Model-Based Predictor-Corrector (MPC)' approach. While executing the planned path both the progress in motion and the NR behaviour itself will be predicted taking into account the current NR state and command set. The comparison of that predicted NR state with the measured one allows fault-detection as well as verification of fault-hypotheses. Additionally a fault-expansion itself can also be extrapolated accordingly to a fault-propagation law (based on the NR characteristics). Such a fault tendency is useful in rating the actual fault-severity.

Having a preliminary fault estimation the corresponding strategy for recovery is executed in order to overcome the problem. This attempt of correction does not guaranty immediate success. May be a set of several iterations will be necessary to locate the real reason of the problem. For that fault analysis ISC takes hold on the complete system state (LS, IH, NR). Additionally it is able to reconfigure system settings for getting a better insight.

In a nutshell: ISC means to look on-line for the first-fitted strategy, which enables the NR to proceed and hopefully to attain the navigation goal.

3.3 Pool of strategies

Typical sources of problems can be divided into three classes:

- Systematic errors within a device characteristic, which can be modeled as well as directly compensated by a local control loop (e.g. track synchronism ...).
- Lack in accuracy or system malfunction due to unmodeled properties, which can or cannot directly be measured (e.g. slippage between NR and soil, especially while turning ...).
- Unpredictable events caused by an accidental combination of trouble sources, which cannot be measured (e.g. being stuck on hitting ground with PLC ...).

For each of them the 'Pool of Strategies (POS)' comprises at least one recovery method. Unfortunately each strategy is highly dependent on both the system characteristic and the system instrumentation. For that reason a detailed strategy description is beyond the scope of the paper.

Just a few common words to the principle of strategy based system intervention:

The superior goal in navigation and therefore the basic strategy is the minimization of the distance to a given point. Compliant to that requirement each methodology is applicable if it supports that goal, keeps given boundary conditions and does not jeopardize the system integrity. The operating costs of a strategy have always to be chosen proportional to the desired quality resp. sys-

tem state and inverse proportional to the remaining control error. In case of a risky ambiguity of results a final decision-maker has to be contacted with a call for help (typically GCS).

Having these rules in mind the proposed set of strategies is split into two categories:

- On-line supervision of NR motion tendency (reduced accuracy and low computational load).
- Off-line NR localization with maximum precision (no motion allowed while taking measurements) and high computational load.

Finally a short excerpt out of POS, which gives a better impression of typical actions managed by a strategy:

- Reconfiguration of NR kinematics to improve visibility of the features within the localization process.
- Adaptation of system parameter wrt. the progress in the navigation process (e.g. Overshoot avoidance ...).
- Overcome obstacles which causes local disturbances.

3.4 Principle of NR position correction

Whatever strategy has been selected as a hard and fast rule the NR will be reoriented first towards the next way point via extra rotational commands and high precision result verification. Thereafter the NR automatically proceeds its linear trek to the next way point (Figure 4: Computed path correction). The reason for that sequential procedure is explained by the high intrinsic sensitivity of NR motion to angular errors.

The control itself focuses on the dominant degrees of freedom x_{trans} , y_{trans} (i.e. parallel to the surface) and z_{rot} (perpendicular to the surface) defined in surface coordinates. The remaining degrees of freedom are supervised only to detect critical situations (via ISC). Each time getting a new NR position, the running motion command will be superimposed by a new command taking into account the current deviation from the planned path. This control concept guarantees, that the NR motion will be iteratively redirected towards the next way point while traversing a path segment (Figure 4). A path segment has been successfully finished as soon as the NR has reached a predefined tolerance zone at its end.

4 Image Processing

The most important point throughout navigation is the precise localization of NR. According to the PSPE instrumentation a vision-based 3D localization technique is proposed. Because IH based applications are typically scheduled for the very beginning of planetary exploration, the reuse of the IH for navigation is an attractive utilization of free LS resources later on. Moreover a typical IH characteristic chosen for scientific usage does also fit the navigation requirements.

In case of vision-based localization there are two possible methods for feature extraction:

- A 'Passive Feature (PF)' concept, which allows a

most probable recognition of pattern primitives as edges, corners, circles etc. doing a statistical image evaluation.

- An 'Active Marker (AM)' concept, which yields a most probable identification of synthetic on-off features in a sequence of camera views.

	PF	AM
Computational load	high	low
Image segmentation	complex	simple
Sensitive to	Illumination	Marker properties
Result quality	fail-safe	accident sensitive

As soon as the feature extraction has been finished, an appropriate method for model-based 3D pose estimation has to be executed [9][10].

Due to the limitations of an operational system for a real mission scenario, the AM concept is preferred because of its lower computational load. The following section describes the AM detection and chapter 5 the proposed NR localization method in more detail.

4.1 Principle of AM localization method

As a mandatory extension to the basic configuration, a set of 4 AM's was mounted on top of PLC (Figure 3: LED's) at well-known coordinates. They are used as individually controllable light beacons within the scope of feature detection. The detection method itself bases on a set of two sequential images representing the same scene with unchanged camera view, but with different AM state (flashing and not flashing). Assuming a strong contrast between the flashing and non flashing marker, a 'Difference Image Analysis (DIA)' yields the location of the marker in the coordinates of the considered camera head.

Moreover the critical correspondence problem in the field of stereoscopic image evaluation is drastically simplified due to the apriori known, local identity of a punctual synthetic feature within the view of both cameras. I.e. the feature detection method is simply executed twice, for each camera independently, with the same AM flashing sequence. Later on two corresponding image points in 2D can be converted to an equivalent 3D point via triangulation (back-projection). To do so, the correct knowledge of external and intrinsic parameters of the IH is mandatory. Both are available the intrinsics due to an extensive calibration at pixel level (done by the camera manufacturer DLR-Berlin), as well as the externals due to an in-situ calibration using the assembled IH as it is (done by KU-Leuven [8]).

The drawback of the AM concept is its accident-sensitivity and the large number of necessary images, taken one by one at different points in time: 1 reference image and 4 individual AM images. I.e. at least 5 im-

ages for each camera. For the whole sequence a comparable image characteristic has to be guaranteed. As shown in Figure 5 the AM detection is therefore subdivided into 3 steps:

- First, a ‘Region of Interest (**ROI**)’ will be defined, which reduces the load of handling huge images. Moreover the most probable NR location is centered by the IH via an electrical follow-up (PTU).
- Second, potential AM’s will be extracted from the selected ROI. Due to the accident-sensitive DIA the quality and similarity of processed images has to be monitored in order to minimize disturbances and accentuate possible AM candidates.
- Third, the set of potential AM’s is subjected to a plausibility check considering general model-based interdependencies.

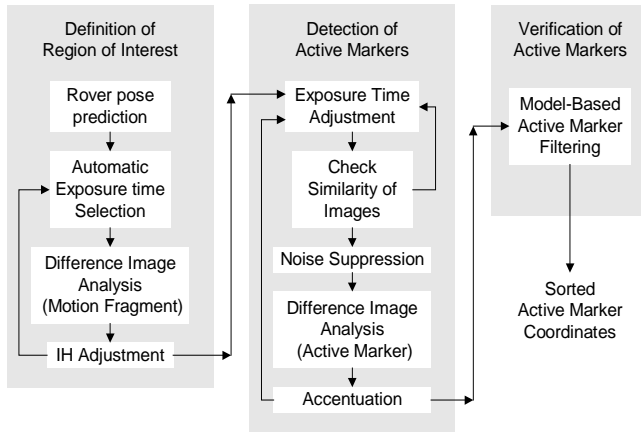


Figure 5: Control flow of AM detection.

A robust method to extract interesting regions of an image bases on the ‘Motion Fragment Analysis (**MFA**)’. The technique behind is equivalent to the AM concept, but in this case the NR itself is considered to be a big AM. A DIA of two images with different NR position bears noticeable traces of its motion. In such a situation morphological filtering as well as standards in the field of ‘Blob Analysis (**BA**)’ are optimal tools to define the region of highest probability where the NR could be. The computational load is quite low and allows an on-line follow-up (e.g. by the PTU). Even big disturbances like unexpected vibrations of the IH while taking an image does not waste the result completely as long as the motion fragment density distribution masses close to the real NR location.

Different for the MFA, which is applicable only as a tendency measure, the AM concept has to bring out at best absolute image coordinates of each AM within sub-pixel resolution. Furthermore the acquirable detection accuracy must not be influenced by the current constellation of the IH and the NR. For that reason the basic form of an AM has to be both compact and symmetric.

Due to this geometrical constraint pixel-based filter operations (e.g. morphological, if applicable) does not distort the interesting focal point of an AM in a wide range.

4.2 Limits of AM localization method.

Several additive effects have a negative influence on the visibility of an AM. The order of magnitude is direct proportional to the distance:

- A small inclination angle of the IH, which is a typical indicator of a huge AM distance, complicates the visibility as well as separability of PLC mounted AM’s.
- CCD blurring caused by local overexposure of pixels adulterates the results of DIA (section 4.1).
- Changes concerning the illumination soften the contrast or produce reflections within a sequence of images. For both the discriminatory power of the DIA result degrades.
- The signal-to-noise ratio (**SNR**) per DIA goes rapidly down and reaches in a distance of approx. 7.5 meters the value 1. I.e. pixel noise produces equivalent results as a real AM. At least at that point the usage of any kind of morphological filtering has completely become senseless.
- Pixel quantization in combination with a small inclination angle causes big uncertainties during the ongoing localization process especially in case of the depth resolution.

These limits can partly be managed by a work-around, typically a reconfiguration, which results in a better system representation (e.g. section 3.3: Strategy to improve AM visibility via a change in current NR configuration). Or by using model knowledge of the system during data evaluation. But that is not possible for all of them.

Distance CCD to AM [m]	1.6	7.5	10.0	20.0
Size of AM [pixel]	25.0	1.0	0.6	0.15

Table 3: AM size depending on the distance to CCD.

Table 3 indicates the most dominant problem immanent to the AM concept, which cannot be manipulated. With increasing distance between AM and camera both detected marker size and intensity decreases in a quadratic order. Finally at the claimed maximum distance - under PSPE project constraints - one AM illuminates at most 15% of a CCD pixel, which makes a reliable AM detection quite unrealistic.

For this extreme situation a change to PF based localization is recommended for more reliable results. The PF advantage over AM is caused by a more universal approach taking into account non-ambiguous silhouettes of NR. But it costs a noticeable rise of the computational load which has to be managed by the LS computer. For sure also PF has a maximum localization depth, but it is certainly beyond the given project re-

quirement.

4.3 Automatic Follow-up of the stereoscopic range .

A very important point - not to be sneezed at - in the autonomous navigation concept is the automatic alignment and follow-up capability of the IH wrt. the NR movements. At any point in time NR should be focused close to the middle of the stereoscopic camera range. But a simple evaluation of both mono-images is not sufficient for that purpose.

Distance [m]	1.6	10.0	20.0
Mono camera range [m]	0.65	4.10	8.20
Stereoscopic coverage [m]	0.44	2.78	5.06

Table 4: Stereoscopic coverage (see also Table 1).

In addition to the consideration of a pure stereoscopic aspects, an error model of the effective IH setup has to be taken into account. The parameter of this model were typically identified during vision-based terrain exploration at the very beginning. Both predicted and measured NR locations can be used to align the IH precisely.

5 Vision-Based Pose Estimation

The core problem doing a ‘Model-based 3D Pose Estimation (MPE)’ is to adjust the position and orientation of an appropriate object model, defined in an ‘Object Coordinate System (OCS)’, with measured features of a real object in a ‘Sensor Coordinate System (SCS)’. Typically a wide-range of equivalent object models can be designed for the same object as long as the selected set of features supports an unique alignment. But the design process is certainly limited to features, which will be optimal in combination with the available measuring equipment. In principle a model-based approach is a reliable and fail-safe method especially in case of redundant or ambiguous information. And it is easy to add different qualities of information to the model in the sense of a sensor fusion concept.

Due to the nature of the problem this pose estimation approach is divided into two complementary steps:

- First, we apply an analytical linear approach, which delivers a first guess of the NR’s pose in a numerically efficient way, but not optimal in terms of any error criterion.
- Second, we use a more accurate nonlinear approach starting with this initial guess for an iterative improvement in the sense of least-squares estimation. The same image acquisition model will be applied to both steps.

5.1 Image acquisition model

The NR, whose pose should be located, is represented by an object model $X_{<OCS>}$ which consists of n markers (AM’s) expressed in homogeneous coordinates wrt.

an object coordinate system.

$$X_{<OCS>} \hat{=} \begin{bmatrix} x_{11} & \dots & x_{1n} \\ x_{21} & \dots & x_{2n} \\ x_{31} & \dots & x_{3n} \\ 1 & \dots & 1 \end{bmatrix}$$

In order to simplify the mathematical representation, the origin of the object’s coordinate system is put in the plane, spanned by the markers. And the z-axis of the object’s coordinate system is aligned to be perpendicular to that plane. In this special case the 3rd line of $X_{<OCS>}$ becomes to zero, i.e. $x_{3i} = 0, i = 1 \dots n$.

The transformation from OCS to SCS is modeled by the 3x4 homogenous matrix $A \hat{=} [R, t]$ with the rotational matrix R and the translational vector t . This matrix represents the unknown object pose wrt. the SCS.

$$\begin{bmatrix} y_{11} & \dots & y_{1n} \\ y_{21} & \dots & y_{2n} \\ y_{31} & \dots & y_{3n} \end{bmatrix} = \begin{bmatrix} r_{11} & r_{12} & r_{13} & t_1 \\ r_{21} & r_{22} & r_{23} & t_2 \\ r_{31} & r_{32} & r_{33} & t_3 \end{bmatrix} * \begin{bmatrix} x_{11} & \dots & x_{1n} \\ x_{21} & \dots & x_{2n} \\ x_{31} & \dots & x_{3n} \\ 1 & \dots & 1 \end{bmatrix} \quad (1)$$

$$Y_{<SCS>} = A * X_{<OCS>}$$

And finally the projection of $Y_{<SCS>}$ from 3D SCS into 2D ‘Image Plane Coordinates (IPC)’ of the left camera ($U_L \in \mathfrak{R}^2$) and the right camera ($U_R \in \mathfrak{R}^2$) is described by the nonlinear equations:

$$\begin{aligned} U_{L<IPC>} &= f_L(L_c * Y_{<SCS>}), \\ U_{R<IPC>} &= f_R(R_c * Y_{<SCS>}). \end{aligned} \quad (2)$$

Thereby $L_c, R_c \in \mathfrak{R}^{3 \times 4}$ are known error matrices, which represent the ‘exterior orientations’ of the left (L) and right (R) camera wrt. the sensor coordinate system. $f_L(\dots)$ and $f_R(\dots)$ represent the nonlinear ‘pin-hole camera’ models with the known ‘interior orientations’ including lens distortions.

5.2 Analytical initial guess

The goal is to find definitely an unique approximation of the unknown object pose A (1). In order to solve that linear equation, $Y_{<SCS>}$ will be interpreted as observation. This observation is computed from measurements of the real markers localized by the image processing module and expressed in IPC. The applied computation is basically the inversion of (2). A so-called back-projection maps the stereoscopic IPC into their corresponding 3D representation in the SCS. The result can be considered as an estimate of $Y_{<SCS>}$, which will be used to derive an estimate for A , within one step,

$$A = YX^T(XX^T)^{-1} \text{ for } \text{rank}(X) = 4. \quad (3)$$

But in case of coplanar markers, as obtained by the

selected marker layout applied to the NR, the $rank(X)$ becomes 3. In this situation the special selection of the object coordinate system, as mentioned before, allows a cut of the 3rd row of $X_{<OCS>}$ as well as of the 3rd column of A without loss of information. This elimination results in a problem of reduced dimension, expressed by

$$Y_{<SCS>} = \tilde{A} * \tilde{X}_{<OCS>} \quad (4)$$

$$\text{with } \tilde{A} = \begin{bmatrix} r_{11} & r_{12} & t_1 \\ r_{21} & r_{22} & t_2 \\ r_{31} & r_{32} & t_3 \end{bmatrix} \text{ and } \tilde{X}_{<OCS>} = \begin{bmatrix} x_{11} & \dots & x_{1n} \\ x_{21} & \dots & x_{2n} \\ 1 & \dots & 1 \end{bmatrix},$$

which yields the reduced estimate of \tilde{A} by

$$\tilde{A} = Y\tilde{X}^T(\tilde{X}\tilde{X}^T)^{-1} \triangleq [\tilde{R}, t] \quad (5).$$

This solution delivers the first two columns of R and the translational vector t . The 3rd column of R can be easily calculated by the cross product of the first two columns of R .

This analytical method has the advantage, that \tilde{A} can be determined very efficiently in terms of computational costs. But it does not respect the following constraints:

- *feature dependence*: In reality the markers of the chosen object model are subjected to a rigid body constraint. Therefore the markers are not independent among each other. But applying the back-projection, the corresponding markers are treated as independent.
- *orthonormality*: The rotational matrix R has to be orthonormal. But the result of (5) does not necessarily guarantee its orthonormality. Therefore the object pose $A = [R, t]$, determined by this analytical approach, will normally not result in an accurate solution for our pose estimation problem.

But this approach is sufficient to get an initial guess for the following iterative improvement.

5.3 Iterative improvement

We apply again the object model, as described in 5.1. But now the above mentioned constraints will be considered.

The interdependence of the markers (in 3D-space) will be implicitly taken into account by doing the iterative improvement within IPC, simultaneously. This results in a measurement vector

$$U_{L_c, R_c <IPC>} \triangleq [u_{1L_c} v_{1L_c} \dots u_{nL_c} v_{nL_c}, u_{1R_c} v_{1R_c} \dots u_{nR_c} v_{nR_c}]^T \quad (6)$$

and satisfies the constraint of a rigid object geometry. Additionally, the unknown object pose will not be described by a homogenous matrix of 3x4 independent elements anymore, but by a minimal pose vector

$$p_{<SCS>} \triangleq (\alpha \ \beta \ \gamma \ t_x \ t_y \ t_z)^T. \quad (7)$$

Within this definition the $\alpha \ \beta \ \gamma$ angles represents the

rotational and $t_x \ t_y \ t_z$ the translational part of the object pose in the SCS. In addition the angles $\alpha \ \beta \ \gamma$ describe a rotation matrix R , which fulfils the orthonormality constraint. For example:

$$R_{Euler} \triangleq R_z(\alpha) * R_x(\beta) * R_z(\gamma). \quad (8)$$

Due to the usage of (8) and the focus on IPC, the estimation problem (1) changes to a nonlinear one. So (1) and (2) will be rewritten in a more compact form considering definition (6) and (7):

$$U_{L_c, R_c <IPC>} = f(p_{<SCS>}). \quad (9)$$

Whereas $f(\dots)$ is a known nonlinear projection function from SCS to IPC comprising (1) and (2). For further computation the necessarily performed linearization of (9) results in an overdetermined system of equations

$$\Delta U_{L_c, R_c <IPC>_k} = J_k^{4n \times 6} * \Delta p_{<SCS>_k}, k = 1, 2, 3, \dots, \quad (10)$$

where $J_k^{4n \times 6}$ is the Jacobian matrix at the current pose estimate. $\Delta U_{L_c, R_c <IPC>_k}$, the so-called residuum, is the difference between the current measurement vector and the simulated ones. $\Delta p_{<SCS>_k}$ is the difference between the improved pose estimation and the former one.

And finally (10) will be solved in the sense of least squares using the pseudoinverse of $J_k^{4n \times 6}$:

$$p_{<SCS>_{k+1}} = p_{<SCS>_k} + (J_k^T J_k)^{-1} J_k^T * \Delta U_{L_c, R_c <IPC>_k}, \quad k = 1, 2, 3, \dots \quad (11)$$

In order to obtain the Jacobian matrix (10) - necessary in (11) -, the differentials of $J_k^{4n \times 6}$ are approximated by double sided differences for numerical convenience.

However before the iterative improvement (11) of the pose estimation can be started, the initial guess \tilde{A} of section 5.2 has to be converted to an equivalent pose vector $p_{<SCS>}$ (7). Due to the missing orthonormality of \tilde{A} , an explicit matrix ortho-normalization is recommendable, which improves the quality of the initial pose vector.

The iteration process will be repeated, while the pose corrections $|\Delta p_{<SCS>_{k+1}} - \Delta p_{<SCS>_k}|$ does not fall below a given limit.

First experimental results, gained by the iterative improvement approach, clearly indicate a reduction of the remaining pose-error. Another possibility, bringing substantial improvement of the pose-accuracy, is to corroborate the pose estimation by direct measurings of some of the pose vector elements (e.g. α, β by NR mounted inclinometers).

6 Conclusion

A control method has been proposed for vision-based supervision and control of a small NR's movements at a remote place in space, e.g. for planetary exploration. The navigation concept is arranged for autonomous execution. It does not require specialized hardware. This autonomous behaviour is the core element of an entire end-to-end control system, which was developed within the Payload Support for Planetary Exploration (PSPE) project funded by ESA. This control system allows scientists and operators to select sites for exploration by the NR in a 3-D model of the terrain surrounding the LS. The GCS automatically determines the optimal NR path to visit these sites in a safe and efficient manner and uploads this information in form of high-level commands. The LS subsequently executes these motion commands in an autonomous way and ensures that the NR reaches its destination as planned. Originally developed for space missions, the system can be adapted to comparable applications on Earth, e.g. for controlling mobile robots in harsh and dangerous environments.

Acknowledgement

This work has been performed under the ESA contract No. 13501/99/NL/PA. We would like to thank all the partners from Space Applications Services (SAS), Belgium, KU Leuven, Belgium, Optidrive, Belgium, DLR Berlin, Germany, von Hoerner & Sulger, Germany, and ESA/ESTEC, The Netherlands, for the fruitful collaboration within this European Project.

References

- [1] <http://science.ksc.nasa.gov/mars/Rover/mission.html>
- [2] R. Volpe, T. Estlin, S. Laubach, C. Olson, J. Balam, "Enhanced Mars Rover Navigation Techniques", in Proc. of the IEEE Int. Conf. on Robotics and Automation, San Francisco, CA, April 2000.
- [3] J. Bresina, G. A. Dorais, K. Golden, D. E. Smith, R. Washington, "Autonomous Rovers for Human Exploration of Mars", in Proc. of the 1st Annual Mars Society Conference, Boulder, CO, August 1998.
- [4] R.G. Bonitz, T.T. Nguyen, W.S. Kim, "The Mars Surveyor '01 Rover and Robotic Arm", in Proc. of the IEEE Aerospace Conference, paper no. 2.0301, March 2000.
- [5] S. Laubach and J.W. Burdick, "An Autonomous Sensor-Based Path-Planner for Planetary MicroRovers", in Proc. of the IEEE Int. Conf. on Robotics and Automation, Detroit, MI, May 1999.
- [6] B. Fontaine, D. Termont, L. Steinicke, M. Pollefeys, M. Vergauwen; R. Moreas, F. Xu, K. Landzettel, M. Steinmetz, B. Brunner, H. Michaelis, T. Behnke, R. Dequeker, P. Degezelle, R. Bertrand and G. Visentin, "Autonomous Operations of a micro-Rover for Geo-Science on Mars", ASTRA Workshop, Noordwijk, The Netherlands, 5-7 December, 2000.
- [7] R. Bertrand and M. van Winnendael, "Nanokhod Micro-Rover Environmental Compatibility Requirements and Design", ASTRA Workshop, Noordwijk, The Netherlands, 5-7 December, 2000.
- [8] M. Vergauwen, M. Pollefeys and Luc Van Gool "Autonomous Operations of a Micro-Rover for Geo-Science on Mars", ASTRA Workshop, Noordwijk, The Netherlands, 5-7 December, 2000.
- [9] K. Arbter, G. Hirzinger, J. Langwald, G.-Q. Wei and P. Wunsch, "Proven Techniques for Robust Visual Servo Control", published in 'Robust Vision for Vision-Based Control of Motion', IEEE Press, New York, 2000, Editor: M. Vincze and G. D. Hager, chapter 9, pages 109 – 125.
- [10] P. Wunsch, "Modellbasierte 3-D Objektlage-schätzung für visuell geregelte Greifvorgänge in der Robotik", Shaker Verlag, Aachen, 1998.
- [11] R. Bertrand, J. Brueckner, M. van Winnendael, and M. Novara, "NANOKHOD – A Micro-Rover to explore the Surface of Mercury", 6th i-SAIRAS, Montreal, Canada, June 18-22, 2001.
- [12] M. Vergauwen, M. Pollefeys, L. van Gool, R. Moreas, F. Xu, H. van Brussel and G. Visentin, "Calibration, Terrain Reconstruction and Path Planning for a Planetary Micro-Rover", 6th i-SAIRAS, Montreal, Canada, June 18-22, 2001.
- [13] L. Steinike, B. Fontaine and G. Visentin, "End-to-End Control System for the Nanokhod Planetary Micro-Rover", 6th i-SAIRAS, Montreal, Canada, June 18-22, 2001.
- [14] E. Tunstel, R. Welch, B. Wilcox, "Embedded control of a miniature science Rover for planetary exploration", in 7th Int. Symp. on Robotics with Applications, WAC'98, Anchorage, Alaska, May 1998.
- [15] Bresina, J., Golden, K., Smith, D.E., Washington, R., "Increased Flexibility and Robustness for Mars Rovers", in Proc. of the 5th i-SAIRAS, Noordwijk, Netherlands, June 01-03, 1999.
- [16] Washington, R., "On-Board Real-Time State and Fault Identification for Rovers", in Proc. of the IEEE Int. Conf. on Robotics and Automation, San Francisco, CA, April 2000.
- [17] T. Huntsberger, T. Kubota, and J. Rose, "Integrated vision/control system for autonomous planetary Rovers," in Proc. IAPR Workshop on Machine Vision Applications, Chiba, Japan, Nov 1998.